MICROSTRUCTURE OF PEROVSKITE LANTHANUM NIOBATE AND TANTALATE THIN FILMS PREPARED BY SOL-GEL METHOD

H. Bruncková, Ľ. Medvecký, J. Ďurišin, E. Múdra, T. Sopčák, A. Kovalčíková, R. Podoba

Abstract

Perovskite lanthanum niobate $La_{1/3}NbO_3$ (LN), lanthanum tantalate $La_{1/3}TaO_3$ (LT) and $La_{1/3}Nb_{1-x}Ta_xO_3$ (LNT, x=0.2) thin films (~200 nm thickness) were prepared by sol-gel/spin-coating process on $Pt/SiO_2/Si$ substrates and annealing at 1100°C. The LN, LT and LNT precursors (sols) of thin films were synthesized using Nb- or Ta-tartrate complexes in ethylene glycol at 130°C. The structural properties and morphology of films were characterized by X-ray diffraction (XRD), Raman spectra and focused ion beam scanning electron microscopy (FIB-SEM). XRD analysis indicated that the LT film on the $Pt/SiO_2/Si$ substrate possessed a single perovskite tetragonal $La_{0.33}TaO_3$ phase, while LN or LNT films contained perovskite orthorhombic $La_{1/3}NbO_3$ (in LN) or tetragonal $La_{1/3}TaO_3$ (in LT) and a small amount of secondary pyrochlore $LaNb_5O_{14}$ at 1100°C. The solid state solubility of LN and LT with a two-phase region was observed in the $La_{0.33}Nb_{0.8}Ta_{0.2}O_3$ composition. The spherical (~80 nm) and needle-like particles up to 1μm in heterogeneous microstructure of LN and LNT thin films and presence homogeneous transparent clusters of spherical nanoparticles (~30 nm) in LT were observed.

Keywords: sol-gel, spin-coating, thin films, $La_{1/3}NbO_3$, $La_{1/3}TaO_3$, perovskite phase, microstructure.

INTRODUCTION

Perovskite niobate of $La_{1/3}NbO_3$ (LN) and tantalate of $La_{1/3}TaO_3$ (LT) based on La rare-earth element represent progressive technological benefits in the form of ferroelectric ceramics and thin films for their dielectric, ferroelectric, electrolytic and magnetic properties enabling application example in microelectromechanical systems (MEMS) and solid oxide fuell cells (SOFC) [1,2].

The orthorhombic structure of $La_{1/3}NbO_3$ first proposed by Roth [3] and perovskite structures based on R described Iyer and Smith [4], then Carrillo et al. [5]. Orthorhombic lattice structure with the NbO_6 octahedra at 25°C is transformed to the tetragonal at 200°C for $La_{1/3}NbO_3$ (LN) [6]. The orthorhombic structure at 25°C is transformed into the tetragonal at 650°C for $La_{1/3}TaO_3$ [7]. Lanthanum niobate-tantalate ($LaNb_{1-x}Ta_xO_3$, LNT) is the solid solution of LN and LT and therefore possesses intermediate properties, which vary with the x=Ta/(Nb+Ta) ratio, from those of LN (x=0) to those of LT (x=1). Characterization of other secondary pyrochlore La niobate-tantalate phases is still in its infancy, with most work being performed by Haugsrud et al. [8]. $LaNbO_4$ has a monoclinic structure and transforms into a tetragonal structure at 500°C. $LaTaO_4$ with monoclinic structure at elevated temperatures transforms into orthorombic and tetragonal structure. The

pyrochlore orthorhombic $LaNb_5O_{14}$ structure consists of two types of Nb–O polyhedra. Especially remarkable are the chains of edge-sharing pentagonal NbO_7 bipyramids, which are interconnected by corner-sharing NbO_6 octahedra [9].

The physical and chemical methods of thin film preparation onto different substrates are known: sputtering, pulsed liquid deposition (PLD), physical vapor deposition (PVD) and chemical solution deposition (CSD, sol-gel). The advantages of sol-gel process are: stoichiometry control, homogenity, low process temperature and low cost. Spin-coating, dip-coating, chemical vapor deposition (CVD) and electrophoretic deposition (EPD) could be included to the methods of deposition of single film layers in sol form. The $LiNb_{1-x}Ta_xO_3$ films with x=0.8 were prepared by the thermal plasma spray CVD at 600°C on Si substrates [10]. Perovskite $(K_{0.5}Na_{0.5})_{0.96}Li_{0.04}(Nb_{0.8}Ta_{0.2})O_3$ thin films were epitaxially grown on $SrTiO_3$ substrates using PLD at 600°C [11]. About 500 nm-thick $KTa_{0.7}Nb_{0.3}O_3$ films were prepared by PLD method [12]. $KTa_{0.65}Nb_{0.35}O_3$ films were prepared by sol-gel processing from alkoxide at 750°C with perovskite phase [13]. In the Pechini method, the citric acid based Nb and Ta are highly stable polymerizable complexes (PC) were applied for the preparation of Y_3NbO_3 and $LiTaO_3$ synthesis [14]. $KTa_{0.65}Nb_{0.35}O_3$ films were prepared by PC sol-gel route using citrate complex at 600°C [15]. The PC method offers approach of depositing of thin films with thickness (~150-800 nm) on different substrates from sols at temperatures lower than in conventional alkoxide sol-gel process.

The present paper describes the modified sol-gel method of the film preparation using polymeric Nb or Ta-tartrate complexes and the phase composition and microstructure formation of 5-layered LN, LNT and LT thin films deposited from adequate sols on the $Pt/SiO_2/Si$ substrates by spin-coating method is evaluated.

EXPERIMENTAL

LN(LT) and LNT films were prepared by modified polymeric complex sol-gel method from $La(NO_3)_3$ and Nb(Ta)-tartrate complex in solvent (ethylene glycol) with a molar ratio of La/Nb(Ta) and La/(Nb+Ta) = 0.33/1.0, by spin-coating on $Pt/SiO_2/Si$ substrates and annealing at 1100°C [16,17]. The polymer Nb(Ta) and (Nb+Ta)-tartrate complexes were synthesized by reaction $NbCl_5$ (dissolved in ethylene glycol and mixed with chelating agent (tartaric acid $C_4H_6O_6$ (TA)) and ethylene glycol ($C_2H_6O_2$ (EG)) at molar ratio TA:EG = 3:1). The mole ratio of La:Nb:Ta = 0.33:0.8:0.2 (for LNT film). Basic three LN, LT, and LNT sols were diluted in stabilizer solution (n-propanol) (0.5 M solutions). The platinized substrates (p-type silicon [100] single-crystal wafer of diameter 50 mm and 270 μm thickness) to deposit the films were used. The Pt (50 nm) electrode layer was sputtered as a bottom electrode. The thickness of SiO_2 layer was 1000 nm. $Pt/SiO_2/Si$ substrates were spin-coated with the sol precursor at 2000 rpm for 30s. Individual (single) film layer was deposited on the substrate with a drying step at 110°C/3 min. The final 5-layered films were annealed at 1100°C/30 min. The average thickness of a single layer was about 30-50 nm.

The phase composition of LN, LNT and LT films was determined by the X-ray diffraction analysis (XRD), (a model X' Pert Pro, Philips, The Netherlands) using CuK_α radiation and Raman spectra were collected by a Raman spectroscopy (HORIBA BX 41TF). The surface and cross-section of LN, LNT and LT thin film microstructures were characterized using focused ion beam scanning electron microscopy (FIB-SEM), (Auriga Compact, Carl Zeiss Germany). Cross sections of thin films were cut with the focused Ga^+ ion beam. All SEM images were collected with secondary electrons to achieve highest resolution and topography contrast.

RESULTS AND DISCUSSION

The XRD diffractograms of 5-layered LN, LNT and LT thin films deposited on $Pt/SiO_2/Si$ substrates and annealed at 1100°C are shown in Fig.1. XRD analyses verified formation of the perovskite orthorhombic $La_{0.33}NbO_3$ (JCPDS 35-1298), tetragonal $La_{0.33}TaO_3$ (JCPDS 42-0061) and pyrochlore orthorhombic $LaNb_5O_{14}$ (JCPDS 76-0263) phases. From XRD diffractograms resulted that the major components represent the perovskite $La_{0.33}NbO_3$ (in LN) or $La_{0.33}TaO_3$ (in LT) and traces of pyrochlore $LaNb_5O_{14}$ phase were revealed in both films after annealing at 1100°C. Created pure $La_{0.33}TaO_3$ perovskite phase exhibits a tetragonal superstructure, in which two of the La-sites should remain vacant in LT films [18]. In the experiments, the possible chemical reactions (1) and (2) for the preparation of LN and LT films can be expressed, respectively:

$$LaNbO_4 + Nb_2O_5 + LaNb_5O_{14} \xrightarrow{1000°C} 2LaNb_5O_{14} + LaNbO_4 \xrightarrow{1100°C} 6La_{0.33}NbO_3 + LaNb_5O_{14} \quad (1)$$

$$La_{4.67}Ta_{22}O_{62} \xrightarrow{1000°C} 3LaTa_7O_{19} + LaTaO_4 \xrightarrow{1100°C} 22La_{0.33}TaO_3 \quad (2)$$

The transformation process started from 550°C, where the amorphous niobate $LaNbO_4$ and tantalate $La_{4.67}Ta_{22}O_{62}$ phases were created in LN and LT films, respectively [16,17]. After annealing at 1100°C, the clearly perovskite $La_{0.33}NbO_3$ (in LN) or $La_{0.33}TaO_3$ (LT) crystallized, but some fraction of the pyrochlore $LaNb_5O_{14}$ phase in patterns (in LN and LNT) was found.

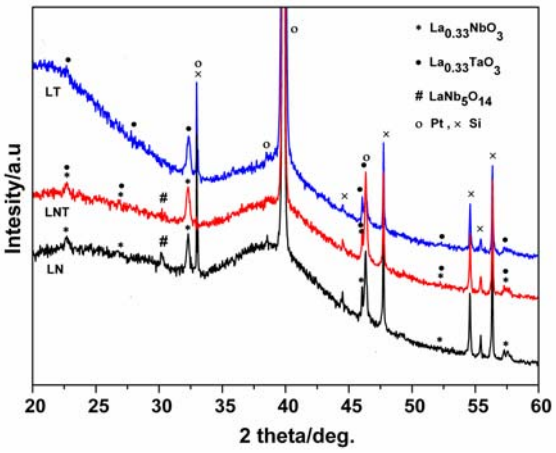

Fig.1. XRD patterns of perovskite 5-layered LN, LNT and LT thin films annealed at 1100°C for 30 min.

Figure 2 shows the Raman spectra of the LN, LNT and LT films deposited on $Pt/SiO_2/Si$ substrates after annealing at 1100°C. Generally, the Raman peaks from the films were similar to those obtained from the powder precursors [16,17]. Two dominant bands at 295 cm^{-1} and 930-980 cm^{-1} were clearly identified in all films. These two bands are assigned as the bending and stretching modes of the BO_6 ($B=Nb^{5+}$, Ta^{5+}) octahedral, respectively [19]. The intense sharp peak at 645 cm^{-1} is visible in LN, contrary at broad band at 625 cm^{-1} in LNT and two small peaks at 605 and 650 cm^{-1} in LT, respectively. The Raman peaks were assigned according to Laguna and Sanjuán (LN) [20] and Noked [21].

The frequencies in the range 230-450 cm^{-1} are influenced by La cation displacements. The 550-850 cm^{-1} range in spectra could be assigned to the Nb-O or Ta-O stretching modes essentially involving oxygen atom shifts.

The surface FIB-SEM microstructures of the LN, LNT and LT thin films are shown in Fig.3. Figure 3 illustrates the effect of the Nb and Ta composition on the morphology. In the LN and LNT films show straight and long cracks similar to those observed by Chen [22] and Zanetti [23] for perovskite $BaTiO_3$ and $SrTiO_3$ prepared by sol-gel method. LN film (Fig.3a,b) with cracks (5 μm) formed during sintering have heterogenous microstructure, in which two different particle forms the large compact particle clusters (composed of fine particles ~80 nm) and coarse rectangular and irregular needle-like shaped particles (~1 μm). The microporores with size in the range of ~200 nm are loaded between rectangular and needle-like particles.

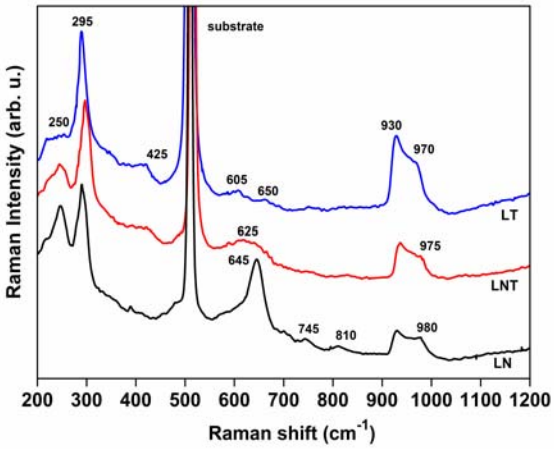

Fig.2. Raman spectra of perovskite 5-layered LN, LNT and LT thin films annealed at 1100°C for 30 min.

Besides the SEM surface observation of LNT thin film (Fig.3c,d) showed that the bigger needle-like particles (up to 1 μm) are surrounded by fine spherical about 50 nm particles. Heterogeneous LN and LNT microstructures are in agreement with the XRD results (Fig.1). The secondary phase of $LaNb_5O_{14}$ is present as the needle-like particles irregular shape with lenght up to 1 μm surrounded perovskite $La_{0.33}NbO_3$ phase (spherical nanoparticles). The homogeneous transparent clusters of spherical nanoparticles (~30 nm) of perovskite $La_{0.33}TaO_3$ phase were observed in the dense microstructure of LT film (Fig.3e,f). In translucent LT film, the white Pt particles of Pt substrate layer were visible. Thus, the particle morphology in the LN and LNT heterogeneous films on $Pt/SiO_2/Si$ substrates was characterized by the bimodal particle size distribution and LT homogeneous film contained spherical nanoparticles and the particle size was lower in the case of LT film.

In Figure 4, the SEM cross-section microstructures of 5-layered LN, LNT and LT films on $Pt/SiO_2/Si$ substrates annealed at 1100°C are shown. SEM images showing the different stages of producing a cross-section specimen of a thin film using FIB. First an area of film at the edge of the surface is coated with Pt (Fig.4a,c,e). Deposition of a Pt-layer on top of the films was required to protect the film during cross section preparation by focused ion beam milling. The Pt partly penetrated into the pores giving rise to regions of

filled pores below the surface of the films. The SEM image confirms the LN (Fig.4a,b) and LNT (Fig.4c,d) films thickness of around ~250 and 200 nm, respectively. The thicknesses of Pt and SiO_2 layers of substrate were ~ 50 nm and 1 μm, respectively (assigned in Fig.4c). The experimental results in LN and LNT thin films indicate the existence of cracks in individual layers. The cross-section view of LT film (Fig.4e,f) shows that the film thickness of ~150 nm is quite uniform. The LT films exhibited a smooth and crack-free surface, composed from densely packed particles.

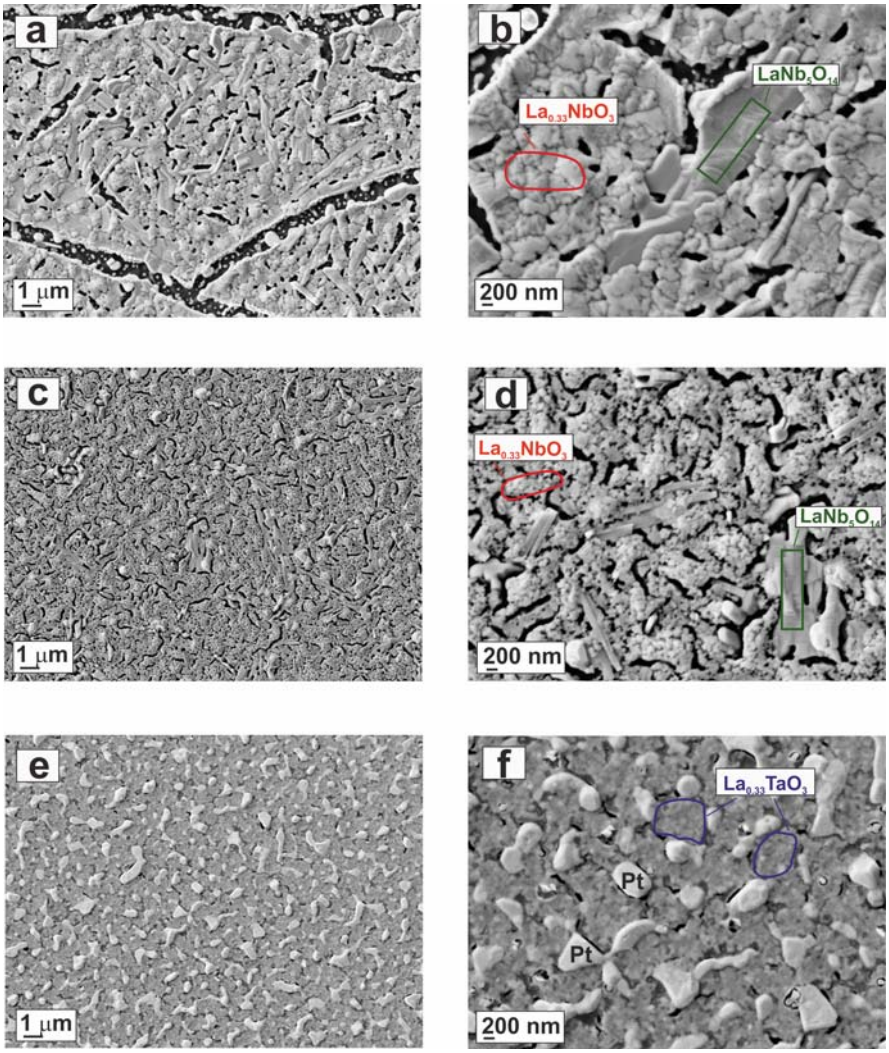

Fig.3. FIB-SEM microstructures of surface of (a,b) LN, (c,d) LNT and (d,f) LT thin films annealed at 1100°C for 30 min.

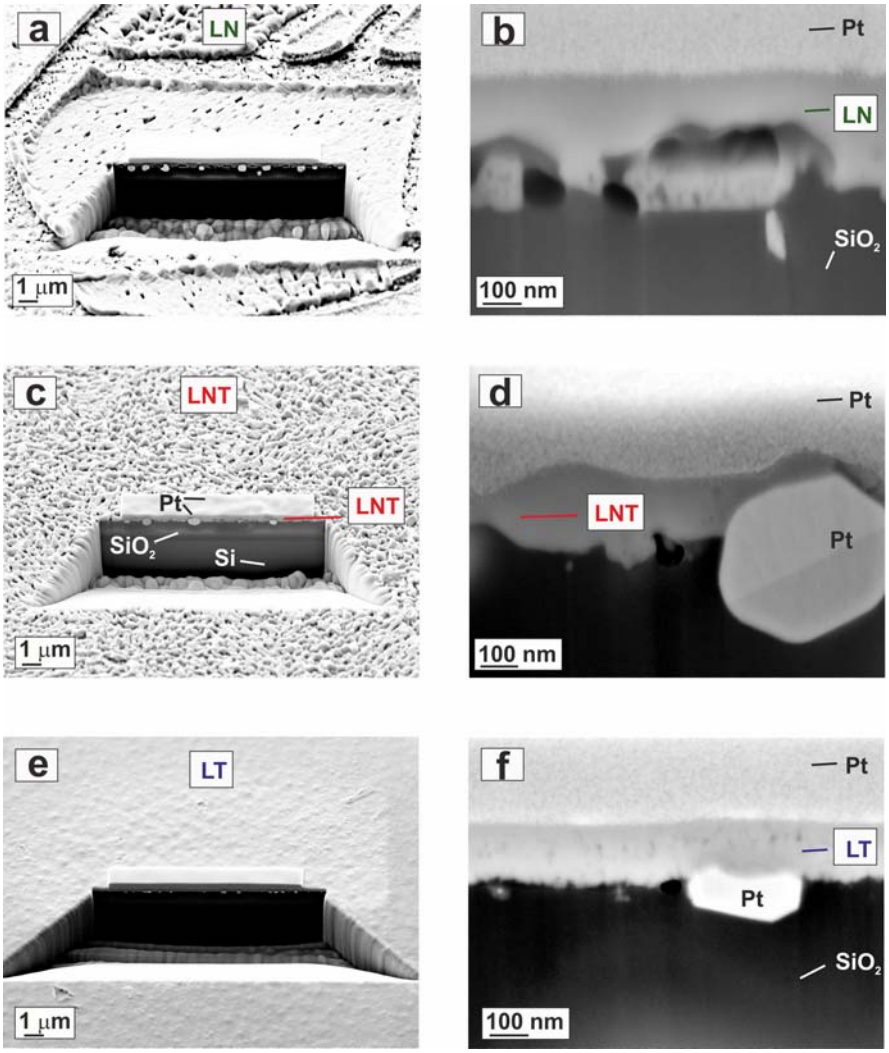

Fig.4. FIB-SEM microstructures of cross-section of (a,b) LN, (c,d) LNT and (d,f) LT thin films annealed at 1100°C for 30 min.

CONCLUSIONS

Perovskite 5-layered $La_{1/3}NbO_3$ (LN), $La_{1/3}Nb_{0.8}Ta_{0.2}O_3$ (LNT) and $La_{1/3}TaO_3$ (LT) thin films were prepared using modified polymeric complex sol-gel method from Nb- or Ta-tartrate sols, which were deposited by spin-coating method on $Pt/SiO_2/Si$ substrates and annealed at 1100°C.

XRD diffractograms revealed the formation of the required perovskite orthorhombic $La_{0.33}NbO_3$ (in LN) or tetragonal $La_{0.33}TaO_3$ (in LNT) phase and traces of the secondary pyrochlore orthorhombic $LaNb_5O_{14}$ (in both films) and pure perovskite tetragonal $La_{0.33}TaO_3$ phase (in LT film).

In the microstructure of LN and LNT thin films, the bimodal particle distribution was observed with the small spherical (~80 nm) and larger needle-like particles (~1 μm) of

the perovskite and pyrochlore phase, respectively. In the transparent compact LT film, clusters composed of fine ~30 nm spherical perovskite particles were found. The long cracks were observed in LN and LNT films and the film thickness of ~200-250 nm was not quite uniform. The LT films with ~150 nm of thickness exhibited a smooth and crack-free surface, composed from densely packed particles.

Acknowledgement

This work was supported by the Grant Agency of the Slovak Academy of Sciences through project No. 2/0041/14.

REFERENCES

[1] Kennedy, BJ., Howard, CHJ., Kubota, Y., Kato, K.: Journal of Solid State Chemistry, vol. 177, 2004, p. 4552
[2] Milkonis, A., Macutkevic, J., Grigalaitis, R., Banys, J., Adomvicius, R., Krotkus, A., Salak, AN., Vyshatko, NP., Khalyavin, DD.: Ferroelectrics, vol. 109, 2009, p. 55
[3] Roth, S.: Rare Earth Research Development. Univ. of California, 1961
[4] Iyer, PN., Smith AJ.: Acta Crystallographica, vol. 23, 1967, p. 740
[5] Carrillo, L., Villafuerte-Castrejon, ME., Gonzáles, G., Sansores, LE.: Journal of Materials Science, vol. 35, 2000, p. 3047
[6] Rooksby, HP., White, EAD., Langston, SA.: Journal of American Ceramic Society, vol. 48, 1965, p. 447
[7] Garcia-Martin, S., Rojo, JM., Tsukamoto, H., Moran, E., Alario-Franco, MA.: Solid State Ionics, vol. 116, p. 411
[8] Hausgrud, R., Norby, T.: Nature Materials, vol. 5, 2006, p. 193
[9] Hofmann, R., Gruehn, R.: Journal of Inorganic and General Chemistry, vol. 583, 1990, p. 223
[10] Kulinich, SA., Yamamoto, H., Shibata, J., Terashima, K., Yoshida, T.: Thin Solid Films, vol. 407, 2002, p. 60
[11] Yao, YB., Chan, HT., Mak, CI., Wong, KH.: Thin Solid Films, vol. 537, 2013, p. 156
[12] Guiller, A., Moussavou, AG., Guilloux-Viry, M., Perin, A., Fopeyrine, J., Sauleau, R., Mahdjoubi, K.: Ferroelectrics, vol. 362, 2008, p. 95
[13] Lu, CJ., Kuang, AX.: Journal of Materials Science, vol. 32, 1997, p. 4421
[14] Tanaka, K., Kakimoto, K., Ohsato, H.: J. Eur. Ceram. Soc., vol. 27, 2007, p. 3591
[15] Simon, Q., Bouquet V., Perrin, A., Guilloux-Viry, M.: Solid State Sciences, vol. 11, 2009, p. 91
[16] Bruncková, H., Medvecký, Ľ., Hvizdoš, P., Girman, V.: Journal of Sol-Gel Science and Technology, vol. 69, 2014, p. 272
[17] Bruncková, H., Medvecký, Ľ., Ďurišin, J., Hvizdoš, P., Girman, V.: Journal of Materials Science, vol. 49, 2014, p. 8423
[18] Yamamoto, A., Uchiyama, H., Tajima, S.: Materials Research Bulletin, vol. 39, 2004, p. 1691
[19] Liu, WC., Zhou, W., Sooryakumar, R., Mak, CL.: Journal of Raman Spectroscopy, vol. 43, 2012, p. 326
[20] Laguna, MA., Sanjuán, ML.: Ferroelectrics, vol. 272, 2002, p. 63
[21] Noked, O., Melchior, A., Shuker, R., Livneh, T., Steininger, R., Kennedy, BJ., Sterer, E.: Journal of Solid State Chemistry, vol. 202, 2013, p. 38
[22] Chen, SY., Chen, IW.: Journal of the American Ceramic Society, vol. 78, 1995, p.2929
[23] Zanetti, SM., Leite, ER., Longo, E., Varela JA.: Applied Organometallic Chemistry, vol. 13, 1999, p. 373